ELSEVIER

Journal of Biomechanics 35 (2002) 1647–1657

JOURNAL OF BIOMECHANICS

www.elsevier.com/locate/jbiomech
www.JBiomech.com

Use of dual Euler angles to quantify the three-dimensional joint motion and its application to the ankle joint complex

Ning Ying, Wangdo Kim*

School of Mechanical & Production Engineering, Nanyang Technological University, 50 Nanyang Avenue, 639798 Singapore

Accepted 17 July 2002

Abstract

This paper presents a modified Euler angles method, dual Euler angles approach, to describe general spatial human joint motions. In dual Euler angles approach, the three-dimensional joint motion is considered as three successive screw motions with respect to the axes of the moving segment coordinate system; accordingly, the screw motion displacements are represented by dual Euler angles. The algorithm for calculating dual Euler angles from coordinates of markers on the moving segment is also provided in this study. As an example, the proposed method is applied to describe motions of ankle joint complex during dorsiflexion–plantarflexion. A Flock of Birds electromagnetic tracking device (FOB) was used to measure joint motion in vivo. Preliminary accuracy tests on a gimbal structure demonstrate that the mean errors of dual Euler angles evaluated by using source data from FOB are less than 1° for rotations and 1 mm for translations, respectively. Based on the pilot study, FOB is feasible for quantifying human joint motions using dual Euler angles approach.

Keywords: Dual Euler angles; Flock of Birds; Joint kinematics; Ankle joint complex; Joint coordinate system

1. Introduction

Studies of three-dimensional joint kinematics are important to orthopedics and rehabilitation medicine, which necessitate unambiguous, quantitative descriptions of spatial joint motions. Various methods such as Euler/Cardan angles (Chao, 1980; Tupling and Pierrynowski, 1987) and screw axis or helical axis (Blankevoort et al., 1990; Kinzel et al., 1972) have been proposed in Biomechanics for the description of three-dimensional joint motions and many attempts on standardization of joint motion have been made (Cole et al., 1993; Woltring, 1994).

In the Euler/Cardan angles method, Cartesian coordinate systems are defined in the fixed and moving segments of a joint. At any joint position, the rotational motion of the moving segment with respect to the fixed segment is represented by three ordered rotation angles about the coordinate axes on the moving segment or on the fixed segment. The magnitudes of the three rotation angles depend on the sequence of rotation. Because only the rotation of the joint can be described by Euler/Cardan angles, an additional three-dimensional vector representing the position of the moving segment coordinate system with respect to the fixed segment coordinate system is required to describe the general spatial joint motion completely. Since the rotation angles are referred to the moving segment coordinate system, the translation has to be described with different coordinate system separately, which dose not facilitate the interpretation of the parameters.

Grood and Suntay (1983) proposed a non-orthogonal joint coordinate system (JCS) to avoid sequence dependency by predefining the axes of rotation. The JCS includes two axes embedded in the fixed and moving segments, respectively, and a floating axis perpendicular to two body-fixed axes. Following the recommended procedure, the rotations about the defined axes correspond to the clinical motions of flexion-extension, adduction–abduction, and internal rotation–external rotation. And the translations along the defined axes correspond to the medial–lateral shift, anteroposterior drawer, and distraction–compression.

*Corresponding author. Tel.: +65-790-6890; fax: +65-792-1859.
E-mail address: mwdkim@ntu.edu.sg (W. Kim).

0021-9290/02/$ - see front matter © 2002 Elsevier Science Ltd. All rights reserved.
PII: S0021-9290(02)00241-5

As a variant of Euler/Cardan angles, singularity may occur in the JCS, that is, some joint postures cannot be defined. Moreover, the JCS is not orthogonal. Non-orthogonality will present a serious problem when joint forces and moments are going to be determined (Zatsiorsky, 1998).

The screw axis method provides the full description of the general spatial joint motion as a rotation about and a translation along an axis (screw axis) in space. Though the screw axis method can represent the general three-dimensional joint motion completely, it is hardly compatible for describing the clinical motion, so it does not facilitate communication between engineers and clinicians.

In this study, a modified Euler angles method—dual Euler angles approach, which has been used in studying mechanical systems (Yang, 1969; Fischer, 1999)—is introduced to describe exact three-dimensional joint motions. A general spatial joint motion is considered as three ordered screw motions with respect to the coordinate axes of the moving segment. These three screw displacements with respect to the coordinate axes are represented by three dual angles, called dual Euler angles, accordingly. The proposed method that is based on the two Cartesian coordinate systems can describe full six-degree-of-freedom joint motion in a way similar to that of the JCS. Motion represented by the dual Euler angles method can also be interpreted in clinical motion pattern as the JCS does. Moreover, the use of Cartesian coordinate system can overcome disadvantages such as non-orthogonality in the JCS.

2. Kinematics background

2.1. Dual Euler angles and dual transformation matrix

Consider a rigid body moving from the initial position, where the local coordinate system M on the rigid body coincides initially with the global coordinate system G, to another position in space by rotating about and translating along the X-axis of G as shown in Fig. 1. The screw motion displacement of the rigid body through the X-axis can be expressed in the form $\hat{\alpha} = \alpha + \varepsilon a$ called dual angle, in which α represents the rotation angle about the X-axis and a represents the translation distance along the X-axis (see Appendix A for algebra).

At the initial position, a vector on the rigid body is expressed in the form $\hat{\mathbf{V}}_0 = \mathbf{V}_0 + \varepsilon\mathbf{W}_0$, where $\mathbf{V}_0$ represents the magnitude and direction of the vector with respect to G, and $\mathbf{W}_0 = \mathbf{r} \times \mathbf{V}_0$. Here $\mathbf{r}$ is a vector connecting the origin of G to any point on the line, on which the vector lies. After the screw motion through the X-axis, the same vector moves to position 2. At the final position, the vector can be represented similarly as

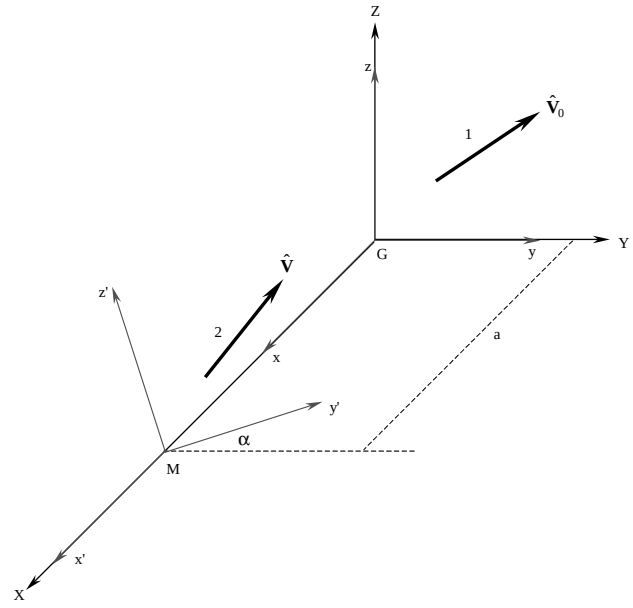

Fig. 1. Screw motion through the X-axis.

$\hat{\mathbf{V}} = \mathbf{V} + \varepsilon\mathbf{W}$. Then the vector satisfies the following dual transformation relationship:

$$\hat{\mathbf{V}} = [\hat{R}_X(\hat{\alpha})]\hat{\mathbf{V}}_0, \tag{2.1}$$

where

$$[\hat{R}_X(\hat{\alpha})] = \begin{bmatrix} 1 & 0 & 0 \\ 0 & \cos\hat{\alpha} & -\sin\hat{\alpha} \\ 0 & \sin\hat{\alpha} & \cos\hat{\alpha} \end{bmatrix}$$

is the dual transformation matrix.

In the same manner, the dual transformation matrices for a screw motion through the Y-axis with a dual angle $\hat{\beta} = \beta + \varepsilon b$ and a screw motion through the Z-axis with a dual angle $\hat{\gamma} = \gamma + \varepsilon c$ are

$$[\hat{R}_Y(\hat{\beta})] = \begin{bmatrix} \cos\hat{\beta} & 0 & \sin\hat{\beta} \\ 0 & 1 & 0 \\ -\sin\hat{\beta} & 0 & \cos\hat{\beta} \end{bmatrix}$$

and

$$[\hat{R}_Z(\hat{\gamma})] = \begin{bmatrix} \cos\hat{\gamma} & -\sin\hat{\gamma} & 0 \\ \sin\hat{\gamma} & \cos\hat{\gamma} & 0 \\ 0 & 0 & 1 \end{bmatrix},$$

respectively.

A general spatial motion of a rigid body moving in space can be considered as three successive screw motions about the axes of the coordinate system on the rigid body or the global coordinate system. And any sequence of screw motions about the axes can be chosen as long as the same axis is not repeated consecutively. The resultant dual transformation matrix $[\hat{R}]$ is the combination of all three dual transformation matrices. For successive transformations with respect to the axes

of the fixed global coordinate system, $[\hat{R}]$ can be obtained by successive left multiplication, and for successive transformations with respect to the axes of the moving rigid body $[\hat{R}]$ can be obtained by successive right multiplication. In this study, screw motions about the coordinate system fixed on the moving segment are used to describe joint motion, and the three dual angles expressing the screw motions about the axes of the moving segment coordinate system are called dual Euler angles.

Similar to Euler angles method, the sequence of screw motions is important in dual Euler angles method. For example, if the sequence of screw motions is chosen as first with respect to the z-axis, then with respect to the new y-axis (y'-axis), and finally with respect to the new x-axis (x''-axis), the resultant dual transformation matrix can be obtained by

$$[\hat{R}] = [\hat{R}_z(\hat{\gamma})][\hat{R}_{y'}(\hat{\beta})][\hat{R}_x(\hat{\alpha})]. \tag{2.2}$$

Similar to the ordinary transformation matrix in Euler angles method, the dual transformation matrix is orthogonal, that is $[\hat{R}][\hat{R}]^{\mathrm{T}} = I$.

2.2. Algorithm for calculating dual transformation matrix from coordinates of points

At present, the dual Euler angles of a rigid body moving in space cannot be measured directly. An approach is developed to obtain the dual transformation matrix and dual Euler angles from measurement data. Generally, the coordinates of n points ($n \geqslant 3$) on the rigid body with respect to a global coordinate system can be obtained from experiments. Because data from experiments contain noise, least-square algorithms are used in this study to calculate the dual transformation matrix of the rigid body from the coordinates of points.

Suppose with respect to the global coordinate system coordinates of n points at the initial position and final position are measured as $\mathbf{r}_{0i}$ and $\mathbf{r}_i (i = 1, 2, 3, \ldots, n)$, respectively. Then the centroids of the points at the initial and final position are $\mathbf{c}_0 = 1/n \sum_{i=1}^{n} \mathbf{r}_{0i}$ and $\mathbf{c} = 1/n \sum_{i=1}^{n} \mathbf{r}_i$, respectively.

According to the dual transformation relationship as introduced above, at the final position the vector connecting the centroid and the ith point can be estimated by $\hat{\mathbf{V}}_i = \tilde{\mathbf{V}}_i + \varepsilon\tilde{\mathbf{W}}_i = [\hat{R}]\hat{\mathbf{V}}_{0i}$, where $\hat{\mathbf{V}}_{0i} = (\mathbf{r}_{0i} - \mathbf{c}_0) + \varepsilon\mathbf{c}_0 \times (\mathbf{r}_{0i} - \mathbf{c}_0)$. On the other hand, at the final position, the same vector can be calculated from measurement data as $\hat{\mathbf{V}}_i = \mathbf{V}_i + \varepsilon\mathbf{W}_i = (\mathbf{r}_i - \mathbf{c}) + \varepsilon\mathbf{c} \times (\mathbf{r}_i - \mathbf{c})$. Because of noise, there is difference between $\hat{\mathbf{V}}_i$ and $\hat{\mathbf{V}}_i$. In the sense of least squares, the dual transformation matrix $[\hat{R}]$ should minimize $J = 1/n \sum_{i=1}^{n} (\|\mathbf{V}_i - \tilde{\mathbf{V}}_i\|^2 + \|\mathbf{W}_i - \tilde{\mathbf{W}}_i\|^2)$. Here $\|\ \|$ is referred to the norm of a three-dimensional vector. This optimization problem subjects to the orthogonal constrain $[\hat{R}][\hat{R}]^{\mathrm{T}} = I$.

This constrain in dual-number matrix form can be expanded into two functions in ordinary matrix form as shown in Eq. (A.8) in Appendix A, from which twelve constrain functions can be obtained. The optimal estimation of the elements in dual transformation matrix were determined by solving the above constraint optimization problem using Sequential Quadratic Programming (SQP) method (Fletcher, 1980). Optimization toolbox in MATLAB (The Math Works, Inc., Natick, MA, USA) was used as a computation tool in this study. Furthermore, the dual Euler angles were obtained based on the relationship between dual Euler angles and dual transformation matrix.

3. Application and testing

An example should suffice to show how the dual Euler angles method can be applied to assess human joint kinematics. In this study the ankle joint complex (AJC) motion was represented using the proposed method. A Flock of Birds electromagnetic tracking system (Ascension Technology, Burlington, Vermont, USA) consisting of a standard range transmitter and three wired sensors was used to measure motions of AJC during dorsiflexion–plantarflexion in vivo. Due to the difficulty in tracking the motion of the talus in vivo, only the overall motion of the ankle-subtalar joint complex, that is, the relative motion of the foot with respect to the shank, was measured in the present study.

Different from other measurement systems, FOB provides both orientation and position of sensors. A special method was used in this study to obtain the coordinates of points on segments.

3.1. Verification of method by Gimbal test

Though some papers have reported the accuracy of position and orientation of FOB (Bottlang et al., 1998; Bull et al., 1998; Meskers et al., 1999), the accuracy of dual Euler angles calculated using source data from FOB has not been determined yet. As a preliminary step for investigating the accuracy of results of in vivo AJC measurements, a gimbal structure as shown in Fig. 2, which can produce a motion with known dual Euler angles, was fabricated. By comparing the estimated dual angles with the prescribed known values, the gimbal tests indicate the accuracy of dual angles obtained using measured data from FOB.

The gimbal consists of three square frames and a base of length 360 mm and width 200 mm. All parts of the gimbal are acrylic or plastic to avoid the distortion effect on the electromagnetic field caused by metallic objects. Frame 1 is supported by an axis fixed on the base and the thread was built in with a pitch of 1.2 mm along the axis. By rotating Frame 1 about its own axis, Frame 1

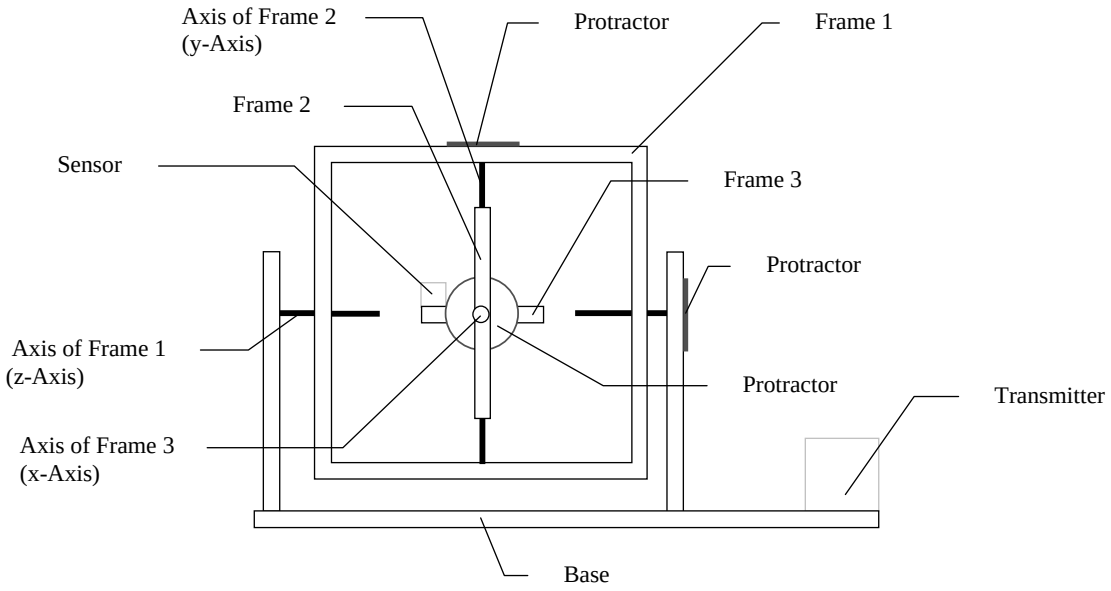

Fig. 2. Experimental setup for accuracy testing.

will move along its axis with the prescribed pitch simultaneously, that is, the motion of Frame 1 can be described as a rotation about and a translation along its axis. In this way, the screw motion can be simulated. Similarly, Frames 2 and 3 can rotate about and translate along their own axes fixed on Frames 1 and 2, respectively. Moving the frames through their axes can generate three known screw motions. Rotation angles of the frames about their own axes can be measured by the three protractors which are attached on the base, Frames 1, and 2, respectively. And translation distances of the frames are determined from the rotation angles and the pitches of threads.

Tests on the gimbal were performed under the default system configuration of FOB: 103 Hz, AC wide filter on, DC low pass filter on, the output with positional resolution of 0.01 in and rotation resolution of 0.01°. Before measurements, the transmitter was aligned on the base and a sensor was mounted on Frame 3. Then the gimbal was adjusted to the initial position, at which the three axes were perpendicular to one another and intersected at a point. At this position, the distance between the sensor and the transmitter was about 265 mm, which was within the optimal range reported by Bull et al. (1998). The fixed global coordinate system is defined by the three axes when the gimbal is at the initial position and the origin is the intersection point of the axes. At the initial position, the moving coordinate system on Frame 3 coincides with the global coordinate system.

The position and orientation of the sensor with respect to the transmitter at the initial position having been recorded, the three frames were rotated about their own axes from -40° to 40° at the uniform interval 5° with the initial translation of 0 mm and the position and orientation of the sensor were recorded at each step. The gimbal rotations can be performed starting from Frames 1 or 3. Because the hierarchy of the nested gimbal has been established as shown in Fig. 2, the final displacement does not depend on the temporal order. Then from the initial position the three frame were rotated about their own axes with 360°, respectively, that is, along their own axes the three frames displaced from the origin with an initial translation of 1.2 mm. The measurements at different rotation angles as described above were repeated. Then the same procedure with the initial translation of 2.4, 3.6, 4.8, 6.0, and 7.2 mm was repeated, respectively.

From measured data the three dual Euler angles of Frame 3 were calculated and compared to the prescribed values. Table 1 gives the overall mean errors and standard deviations of three dual Euler angles. Table 1 indicates that the overall mean errors of rotation angle and translation distance for all three dual angles are less than 1° and 1 mm, respectively.

3.2. Experimental procedure on AJC

After the accuracy of calculating dual Euler angles from FOB source data was evaluated, AJC motions were measured. Four adult volunteers without history of ankle traumas or pathologies served as subjects for this study. Before measurements were taken, a sensor was fixed on the shank; a second sensor was fixed on the lateral side of the heel; the third sensor was attached on a pen as a stylus for digitizing the anatomical points of interest. And four landmarks on the shank—the distal apex of the medial and lateral malleolus (MM, LM), the

Table 1
Overall mean errors of three dual angles

	Mean error	
Dual angle about *z*-axis	Rotation	$0.41 \pm 0.06^\circ$
	Translation	0.52 ± 0.07 mm
Dual angle about *y*-axis	Rotation	$0.47 \pm 0.06^\circ$
	Translation	0.87 ± 0.08 mm
Dual angle about *x*-axis	Rotation	$0.74 \pm 0.05^\circ$
	Translation	0.38 ± 0.03 mm

apex head of the fibula (HF), and the prominence of the tibia tuberosity (TT)—were located by manual palpation and another four non-collinear points on the foot were also marked.

In the electromagnetic field of the transmitter, the subject sat on a chair with the shank fixed on the plane horizontally and the ankle joint in its neutral position (ankle angle is 90°). At this position, the coordinates of the landmarks and markers with respect to the transmitter were digitized as follows: placing the stylus tip at each of the landmarks and markers, then slowly rotating around its endpoint while recording the position and orientation of the sensor on the stylus. The method used in this study is similar to that used by Meskers et al. (1999). At the neutral position, the position and orientation of the sensors attached on the shank and the foot were also recorded.

Following recording the necessary data at the neutral position, we asked the subject to make a dorsiflexion–plantarflexion movement from maximum extension to maximum flexion. During the joint motion, the position and orientation of the sensors attached on the shank and the foot were continuously recorded with respect to the transmitter. The movement was repeated for three times on each subject.

3.3. Data analysis

The anatomical coordinate system of the shank, considered to be fixed, is defined by the four landmarks as follows: the origin is at the midpoint of the line joining MM and LM; the *Y*-axis is orthogonal to the quasifrontal plane defined by the MM, LM and HF; the *Z*-axis is orthogonal to the quasisagittal plane defined by the *Y*-axis and TT; the *X*-axis is the cross product of the *Y*- and *Z*-axis (Fig. 3). At the neutral position, the local coordinate system of the foot coincides initially with that of the shank.

The coordinates of the non-collinear markers on the foot with respect to the shank coordinate system during dorsiflexion–plantarflexion were constructed using coordinate transformations (see Appendix B for details). Then the dual Euler angles of the foot with respect to the shank were calculated using the algorithm as introduced in Section 2.2. The sequence of screw motions was selected as first moving through the *z*-axis,

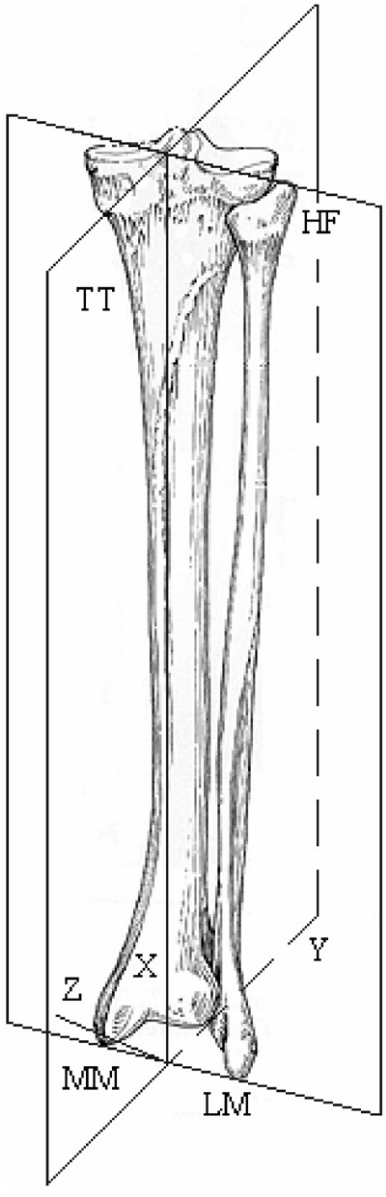

Fig. 3. Anatomical coordinate system of the shank.

then through the new y-axis (y'-axis), and finally through the new x-axis (x''-axis). Before computation, the coordinates were filtered using dynamic programming and generalized cross-validation method to reduce the noise (Dohrmann et al., 1988).

4. Results and discussion

According to the definition of the coordinate systems along with the selected sequence of screw motions adopted in this study, the screw motion through the z-axis can be considered as the flexion–extension and lateral–medial shift of the foot. Similarly, the screw motion through the y' axis reflects the inversion–eversion and anteroposterior drawer of the foot. Finally, the screw motion through the x''-axis can be interpreted as the internal rotation–external rotation and distraction–compression of the foot (Fig. 4).

Fig. 5 shows the dual Euler angles of the foot during dorsiflexion–plantarflexion obtained from three trials on one of the subjects. To compare the parameters obtained from different subjects, the rotation angle about the z-axis was chosen as a reference angle, and the other five parameters—the rotations about the y-axis and x-axis, the translations along the three coordinate axes were examined by varying the reference angle within its range of motion. Fig. 6a demonstrates the kinematic coupling of rotations during dorsiflexion–plantarflexion. And Fig. 6b demonstrates the kinematic coupling of translations. The results show similar kinematic coupling patterns across the different subjects. In addition, as the foot moves from the maximum plantarflexion to maximum dorsiflexion it everts and externally rotates, which agrees with what has been reported by Siegler et al. (1988).

Compared with rotation angles and translations described in the JCS, the dual Euler angles are expressed in orthogonal coordinate systems. If at the neutral position, the two body-fixed axes of the JCS are defined as: the first body-fixed axis is perpendicular to the sagittal plane of the shank, which coincides with the Z-axis; the second body-fixed axis coincides with the x-axis on the foot. The three dual angles through the z-axis, y'-axis, and x''-axis, used in this study, are equivalent to rotation about and translation along the first body-fixed axis, the floating axis, and the second body-fixed axis of JCS, respectively.

But generally at the neutral position, the two body-fixed axes of JCS are not orthogonal to each other, and under this situation, dual Euler angles expressed in cartesian coordinate system cannot be compared directly with rotation angles and translations expressed in non-orthogonal JCS.

Moreover, the dual Euler angles method can avoid the singular position in JCS. As shown in Fig. 7(a), as

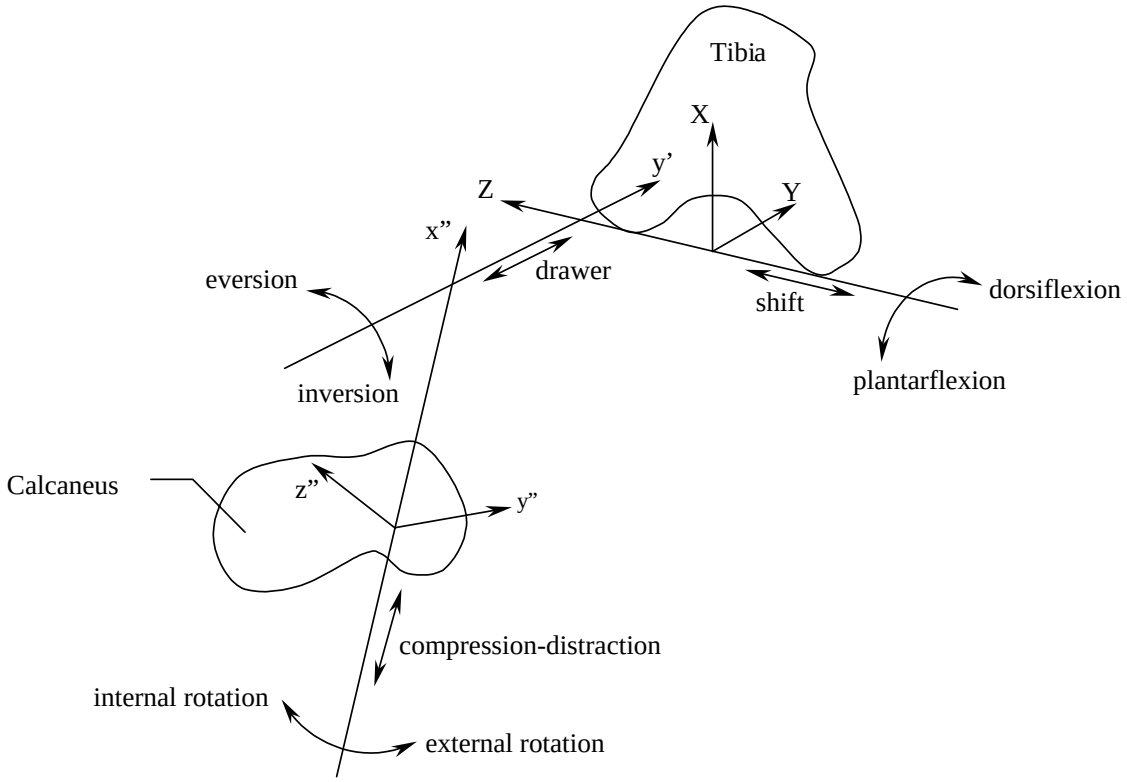

Fig. 4. Screw motions of the foot: (a) dual angle through the z-axis, (b) dual angle through the y'-axis, and (c) dual angle through the x''-axis.

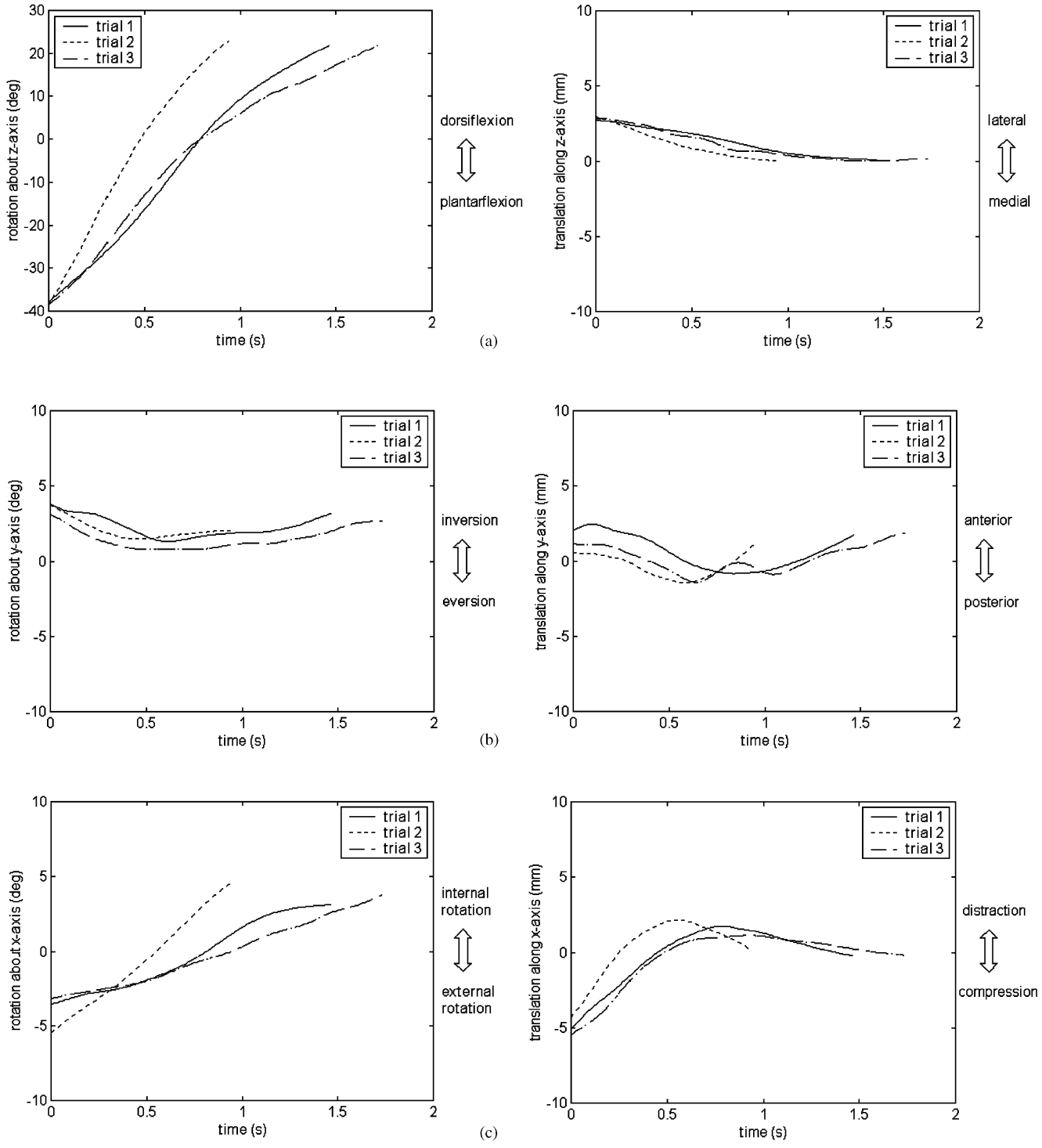

Fig. 5. Dual Euler angles during dorsiflexion–plantarflexion.

the moving segment rotates from the initial position to the final position, where the second body-fixed axis on the moving segment e_3 is collinear with the first body-fixed axis on the fixed segment e_1. Because the cross product of the two vectors cannot be calculated when the two vectors are collinear, the floating axis e_2 is not defined at this position. Such situation may occur when the arm is abducted 90° and the length axis of the arm is collinear with the shoulder frontal axis. The same motion can be described using dual Euler angles methods as first about the z-axis with zero then about the y-axis with $-90°$, and finally about the x-axis with zero as shown in Fig. 7(b).

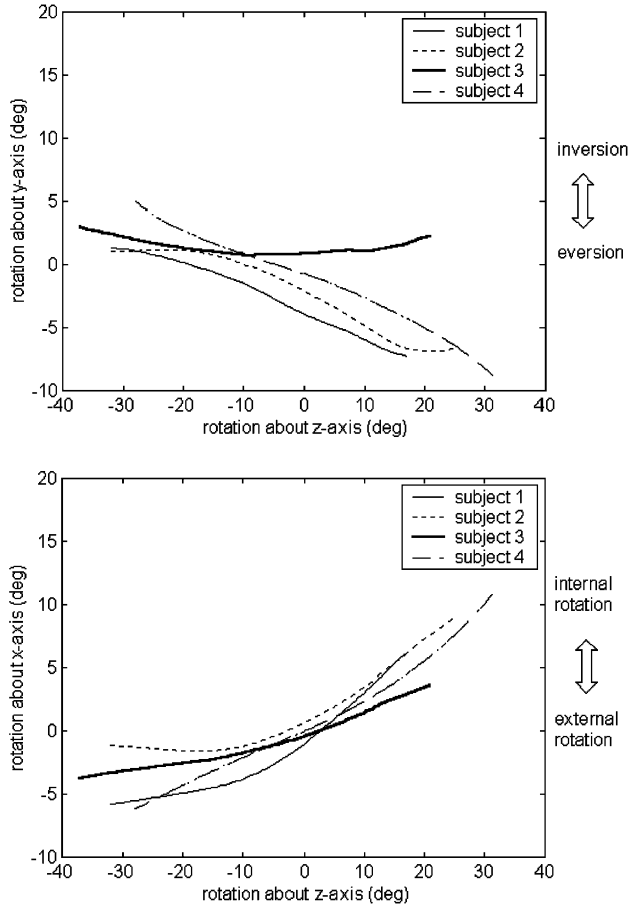

Fig. 6. (a) Kinematic coupling of rotations; and (b) Kinematic coupling of translations.

Since dual Euler angles is an orthogonal system, this orthogonal property can facilitate the solving of problems when joint forces and moments are required to be determined. The concept of three screw motions along the three predefined axes is a convenient way of describing general displacements of joint motion in three-dimensional space. The three motion screws, predefined along human segments in an anatomically meaningful way in this work, can be naturally applied to describe the joint forces by extending the concept to three action screws, the wrench systems (Roth, 1984), which will complete the analysis of the human joint motion in full six-degrees-of-freedom of model.

Similar to the Euler angles method, the proposed method is sequence dependent. The same orientation and position of a segment in space may be characterized by different sets of values depending on the selection of sequence of screw motions. Sequence dependency may cause trouble in comparing the results from different researches unless the sequences of rotations are clearly mentioned.

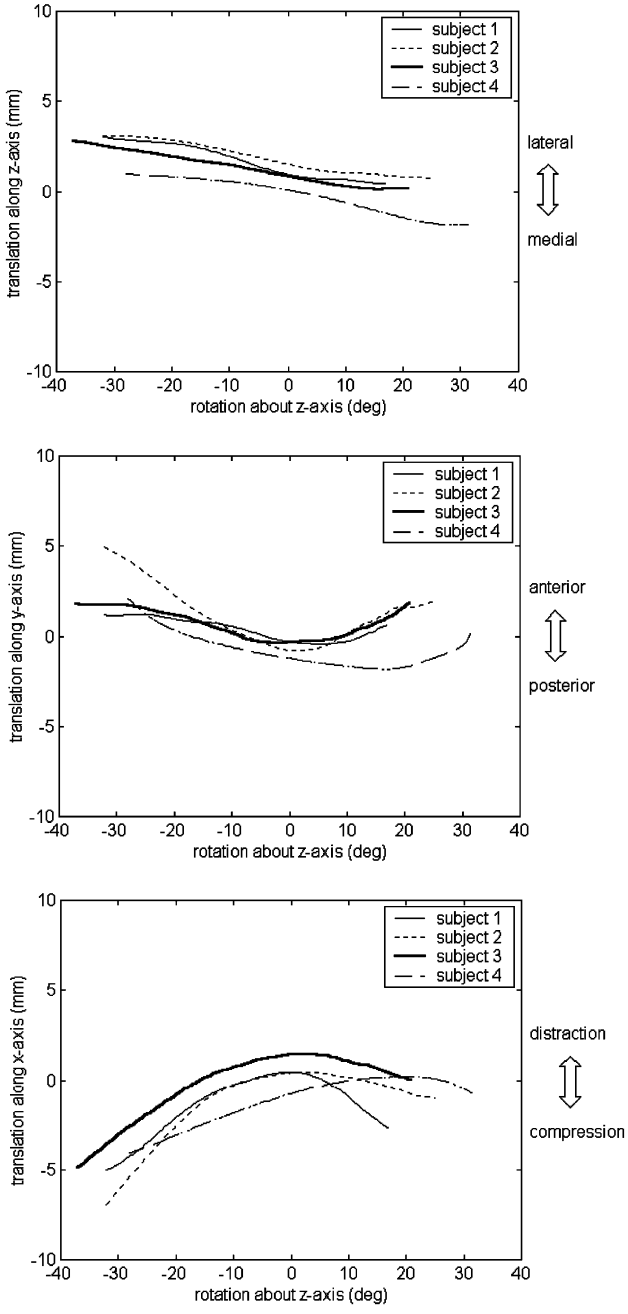

Fig. 6 (*continued*).

5. Conclusion

Compared with Euler/Cardan angles and screw axis methods, dual Euler angles approach provides an alternative way of describing general three-dimensional joint movement, which combines the rotation about and translation along the coordinate axes. The various relationships, such as the orthogonality of transformation matrix in Euler/Cardan angles, also hold in dual Euler angles. Compared with screw parameters, the dual Euler angle method's advantage is that its body

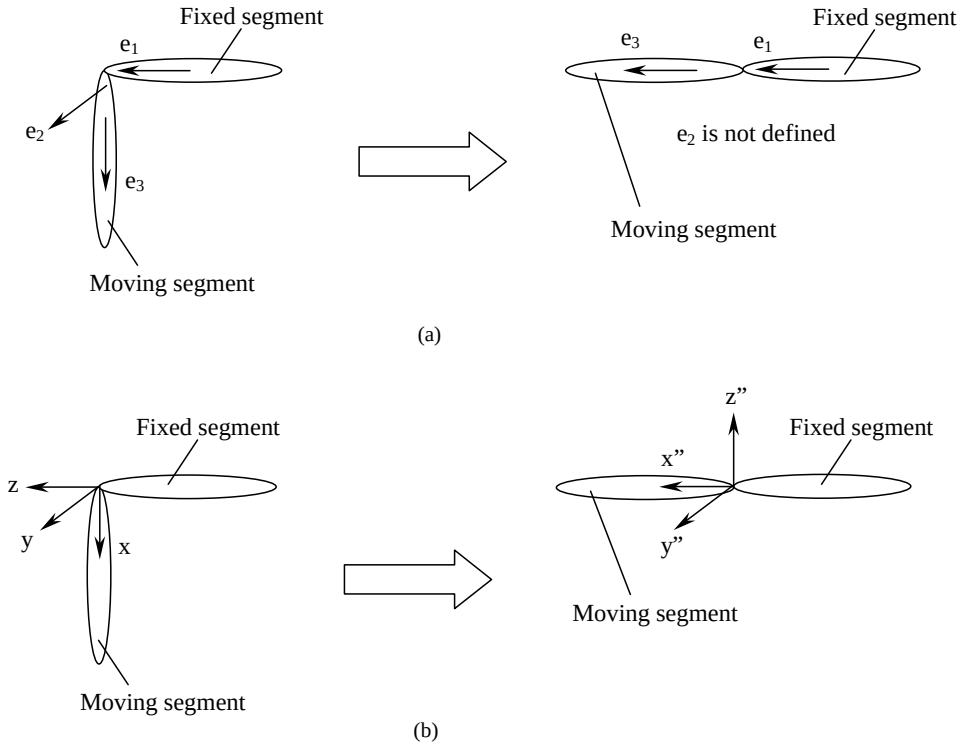

Fig. 7. (a) Joint coordinate system, and (b) dual Euler angles method.

coordinates can be easily understood by clinicians. It has also an advantage over JCS because of its orthogonality. If the sequence of screw motions is selected appropriately, dual Euler angles have the advantage of following anatomical motion pattern.

The accuracy testing results on the gimbal indicate that accurate dual Euler angles can be calculated using source data measured by Flock of Birds electromagnetic measurement system.

Appendix A. Algebra of dual angles and dual transformation

A dual number is defined as $\hat{a} = a + \varepsilon a_0$, where a and a_0 are real numbers, ε is a unit having the property $\varepsilon^2 = 0$. In dual number algebra, addition and subtraction is defined as

$$\hat{a} \pm \hat{b} = (a + \varepsilon a_0) \pm (b + \varepsilon b_0) = (a \pm b) + \varepsilon(a_0 \pm b_0), \quad \text{(A.1)}$$

multiplication is defined as

$$\hat{a}\hat{b} = (a + \varepsilon a_0)(b + \varepsilon b_0) = ab + \varepsilon(ab_0 + a_0 b) \quad \text{(A.2)}$$

and division is defined as

$$\frac{\hat{a}}{\hat{b}} = \frac{a + \varepsilon a_0}{b + \varepsilon b_0} = \frac{a}{b} + \varepsilon \frac{a_0 b - a b_0}{b^2} \; (b \neq 0). \quad \text{(A.3)}$$

For a dual number $\hat{\theta} = \theta + \varepsilon s$ representing the screw motion displacement of a rigid body through a screw axis called dual angle, θ represents the rotation angle about the screw axis and s represents the translation distance along the screw axis. The trigonometric functions of dual angle $\hat{\theta}$ are

$$\begin{aligned} \sin\hat{\theta} &= \sin\theta + \varepsilon s \cos\theta, \\ \cos\hat{\theta} &= \cos\theta - \varepsilon s \sin\theta, \\ \tan\hat{\theta} &= \tan\theta + \varepsilon s \sec^2\theta. \end{aligned} \quad \text{(A.4)}$$

All identities of ordinary trigonometry hold true for dual angles. For example,

$$\begin{aligned} \sin^2\hat{\theta} + \cos^2\hat{\theta} &= 1, \\ \sin 2\hat{\theta} &= 2\sin\hat{\theta}\cos\hat{\theta}, \\ \cos 2\hat{\theta} &= \cos^2\hat{\theta} - \sin^2\hat{\theta}, \\ \tan\left(\frac{\hat{\theta}}{2}\right) &= \frac{1 - \cos\hat{\theta}}{\sin\hat{\theta}}. \end{aligned} \quad \text{(A.5)}$$

As introduced in Section 2.1, a vector on a rigid body satisfies the following dual transformation relationship:

$$\hat{\mathbf{V}} = [\hat{R}]\hat{\mathbf{V}}_0, \quad \text{(A.6)}$$

where $\hat{\mathbf{V}} = \mathbf{V} + \varepsilon\mathbf{W}$, $\hat{\mathbf{V}}_0 = \mathbf{V}_0 + \varepsilon\mathbf{W}_0$, and $[\hat{R}] = [R] + \varepsilon[S]$.

According to the algebra of dual numbers, the above dual form equation can be expanded into the ordinary form as

$$\begin{aligned} \mathbf{V} &= [R]\mathbf{V}_0, \\ \mathbf{W} &= [R]\mathbf{W}_0 + [S]\mathbf{V}_0. \end{aligned} \quad \text{(A.7)}$$

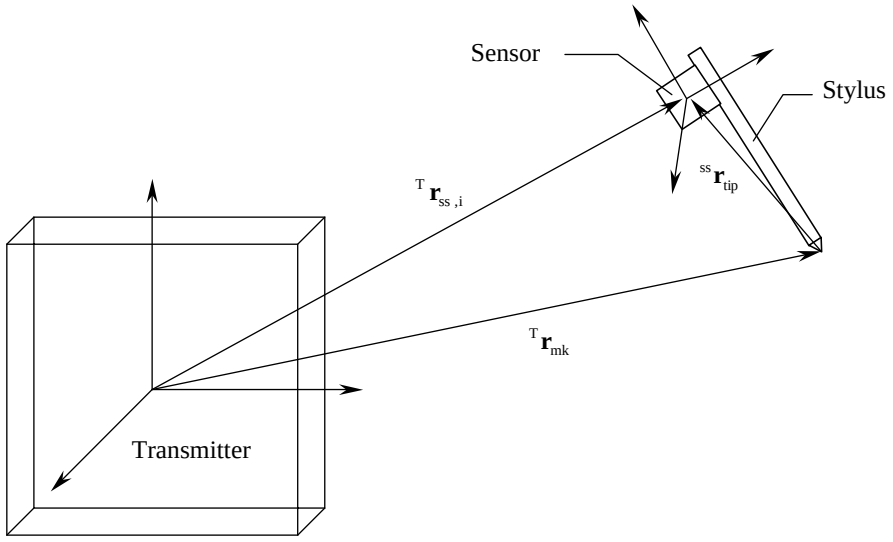

Fig. 8.

And the orthogonal property of the dual transformation matrix can be expressed in the ordinary form as

$$[R][R]^{T} = I,$$
$$[R][S]^{T} + [S][R]^{T} = 0. \quad \text{(A.8)}$$

Appendix B. Coordinates of markers and landmarks

Coordinates of landmarks on the shank and markers on the foot, which are required to compute the dual Euler angles of AJC motion, can be calculated using FOB output as follows.

First, at the neutral position, the coordinates of a landmark or marker with respect to the transmitter $^{T}\mathbf{r}_{mk}$ were calculated using the algorithm to minimize

$$J = \frac{1}{n}\sum_{i=1}^{n} \mathbf{e}_i^{T}\mathbf{e}_i, \quad \text{(B.1)}$$

where $\mathbf{e}_i = [^{T}R_{ss}]_i^{ss}\mathbf{r}_{tip} + ^{T}\mathbf{r}_{mk} - ^{T}\mathbf{r}_{ss,i}$. $[^{T}R_{ss}]_i$ and $^{T}\mathbf{r}_{ss,i}$, obtained from FOB output directly, is the rotation matrix and position vector of the sensor on the stylus with respect to the transmitter. $^{ss}\mathbf{r}_{tip}$ is the vector from the stylus tip to the origin of the sensor's coordinate system described in the coordinate system of the sensor. Fig. 8 graphically shows the symbols used above.

Secondly, once the coordinates of the landmarks at the neutral position are obtained, at the same position the rotation matrix $[^{T}_{N}R]$ and position vector $^{T}_{N}\mathbf{d}$ of the shank coordinate system and the foot coordinate system with respect to the transmitter can be determined. And the coordinates of a marker on the foot with respect to the foot coordinate system can be calculated as

$$^{F}\mathbf{r}_{mk} = [^{T}_{N}R]^{-1}(^{T}\mathbf{r}_{mk} - ^{T}_{N}\mathbf{d}). \quad \text{(B.2)}$$

Finally, during joint motion, the coordinates of the markers on the foot with respect to the shank coordinate system are computed as follows.

At any position the rotation matrix $[^{T}R_S]_i$ and position vector $^{T}\mathbf{d}_{S,i}$ of the shank coordinate system with respect to the transmitter are calculated from

$$[^{T}R_S]_i = [^{T}R_{ss\_S}]_i[^{T}_{N}R_{ss\_S}]^{-1}[^{T}_{N}R],$$
$$^{T}\mathbf{d}_{S,i} = ^{T}\mathbf{d}_{ss\_S,i} - [^{T}R_S]_i[^{T}_{N}R]^{-1}(^{T}_{N}\mathbf{d}_{ss\_S} - ^{T}_{N}\mathbf{d}), \quad \text{(B.3)}$$

where $[^{T}R_{ss\_S}]_i$, $^{T}\mathbf{d}_{ss\_S,i}$ and $[^{T}_{N}R_{ss\_S}]$, $^{T}_{N}\mathbf{d}_{ss\_S}$ represent the rotation matrix and position vector of the sensor on the shank with respect to the transmitter during joint motion and at the neutral position, respectively. These data can be obtained from FOB output.

Similarly, the rotation matrix $[^{T}R_F]_i$ and position vector $^{T}\mathbf{d}_{F,i}$ of the sensor on the foot with respect to the transmitter can also be determined. So during joint motion, at any position the relative orientation and position of the foot with respect to the shank are

$$[^{S}R_F]_i = [^{T}R_F]_i[^{T}R_S]_i^{-1},$$
$$^{S}\mathbf{d}_{F,i} = [^{T}R_S]_i^{-1}(^{T}\mathbf{d}_{F,i} - ^{T}\mathbf{d}_{S,i}). \quad \text{(B.4)}$$

Then the coordinates of the markers on the foot with respect to the shank coordinate system during joint motion can be calculated using the formula

$$^{S}\mathbf{r}_{mk,i} = [^{S}R_F]_i^{F}\mathbf{r}_{mk} + ^{S}\mathbf{d}_{F,i}. \quad \text{(B.5)}$$

References

Blankevoort, L., Huiskes, R., Lange de, A., 1990. Helical axes of passive knee-joint motions. Journal of Biomechanics 23, 1219–1229.

Bottlang, M., Marsh, J.L., Brown, T.D., 1998. Factors influencing accuracy of screw displacement axis detection with a D.C.-based

electromagnetic tracking system. ASME Journal of Biomechanical Engineering 120, 431–435.

Bull, A.M.J., Berkshire, F.H., Amis, A.A., 1998. Accuracy of an electromagnetic measurement device and application to the measurement and description of knee joint motion. Proceedings of the Institute of Mechanical Engineers Part H 212, 347–355.

Chao, E.Y.S., 1980. Justification of the triaxial goniometer in the measurement of joint rotation. Journal of Biomechanics 13, 989–1006.

Cole, G.K, Nigg, B.M., Yeadon, M.R., 1993. Application of the joint coordinate system to three-dimensional joint attitude and movement representation: a standardization proposal. ASME Journal of Biomechanical Engineering 115, 344–349.

Dohrmann, C.R., Bushy, H.R., Trujullo, D.M., 1988. Smoothing noisy data using dynamic programming and generalized cross-validation. ASME Journal of Biomechanical Engineering 110, 37–41.

Fischer, I.S., 1999. Dual-number Methods in Kinematics, Statics and Dynamics. CRC Press, Boca Raton, FL, ISBN 0-8493-9115-6.

Fletcher, R., 1980. Practical Methods of Optimization. Wiley, New York, ISBN 0-471-27711-8.

Grood, E.S., Suntay, W.J., 1983. A joint coordinate system for the clinical description of three-dimensional motions: application to the knee. ASME Journal of Biomechanical Engineering 105, 136–144.

Kinzel, G.L., Hall Jr., A.S., Hillberry, B.M., 1972. Measurement of the total motion between two body segments—I. Analytical development. Journal of Biomechanics 5, 93–105.

Meskers, C.G.M., Fraterman, H., van der Helm, F.C.T., Vermeulen, H.M., Rozing, P.M., 1999. Calibration of the "Flock of Birds" electromagnetic tracking device and its application in shoulder motion studies. Journal of Biomechanics 32, 629–633.

Roth, B., 1984. Screw, motor, and wrench that cannot be bought in a hardware store. Proceedings of the First International Symposium of Robotics Research, pp. 679–693.

Siegler, S., Chen, J., Schneck, C.D., 1988. The three-dimensional kinematics and flexibility characteristics of the human ankle and subtalar joints—Part I: kinematics. ASME Journal of Biomechanical Engineering 110, 364–373.

Tupling, S.J., Pierrynowski, M.R., 1987. Use of Cardan angles to locate rigid bodies in three-dimensional space. Medical and Biological Engineering and Computing 25, 527–532.

Woltring, H.J., 1994. 3-D attitude representation of human joint: a standardization proposal. Journal of Biomechanics 27, 1399–1414.

Yang, A.T., 1969. Displacement analysis of spatial five-link mechanisms using (3×3) matrices with dual-number elements. ASME Journal of Engineering for Industry 91, 152–157.

Zatsiorsky, V.M., 1998. Kinematics of human motion. Human Kinetics, Champaign, ISBN 0-88011-676-5, 100–101.